Progress In Electromagnetics Research B, Vol. 41, 285–305, 2012

ISAR IMAGING OF NON-UNIFORM ROTATION TARGETS WITH LIMITED PULSES VIA COMPRESSED SENSING

J. H. Liu*, X. Li, S. K. Xu, and Z. W. Zhuang

Institute of Space Electronic Technology, School of Electronic Science and Engineering, National University of Defense Technology, Changsha 410073, China

Abstract—This research introduces compressed sensing (CS) principle into inverse synthetic aperture radar (ISAR) imaging of non-uniform rotation targets, and high azimuth resolution can be achieved with limited number of pulses. Firstly, the sparsity of the echoed signal of radar targets with non-uniform rotation in certain matching Fourier domain is analyzed. Then the restricted isometry property (RIP) and incoherence of partial matching Fourier matrices are checked, following which an ISAR imaging method based on CS for both random sparse aperture and short aperture cases is proposed. In particular, considering the dependence of the sparse dictionary on the relative rotation parameter, a parameter estimation method by the optimal search in fractional Fourier domain is presented. Simulation experiments verify the effectiveness as well as superiority of the proposed imaging method over traditional methods in terms of imaging performance.

1. INTRODUCTION

Inverse synthetic aperture radar (ISAR) imaging technique is of great importance in air/space surveillance and ballistic missile defense. Generally, high range resolution is obtained by transmitting wide bandwidth signal and high azimuth resolution is obtained by enough large rotation angle during the coherent processing interval (CPI) [1]. In practice, ISAR targets are usually noncooperative and of strong maneuverability, which may bring great difficulty to the azimuth compression of ISAR imaging for lack of sufficient echo data. In

Received 17 April 2012, Accepted 1 June 2012, Scheduled 11 June 2012

* Corresponding author: Ji Hong Liu (ljh632@163.com).

addition, some pulses may be interfered or used for other radar functions, such as target searching and tracking. All the phenomena may induce incomplete or gapped sampling, which motivates high resolution ISAR imaging methods with very limited pulse echo, and that resolving the contradiction between limited pulse echo and azimuth resolution becomes necessary.

The recently arisen compressed sensing (CS) theory [2, 3] breaks through traditional signal acquisition conception, it argues that sparse or compressible signal can be recovered exactly or approximately via nonlinear optimization from just a few incoherent projections, and has got rapid development in the collection and reconstruction of sparse or compressible signal. It is well known that the electromagnetic characteristics of radar target in high frequency domain can be characterized by a few isolated scattering centers, this provides possibility for the application of CS to radar imaging [4–9]. Recently, the CS-based short aperture and sparse aperture ISAR imaging methods have already attracted extensive attention and made preliminary progress [10–17]. However, all the above-mentioned work are under the assumption that the target's rotation during the CPI is uniform, so the echoed signal in a range cell is composed of single frequency components, and the corresponding sparse dictionary is a discrete Fourier matrix. In fact, the uniform rotation is just a kind of coarse approximation, the non-stationary motion which results in non-uniform rotation often accompanies our interested targets, such as missiles and aircraft with high speed or maneuverability, and warships with complex pendulum motion. In this instance, the echoed signal cannot achieve energy concentration in Fourier domain [18].

In general, the CPI of ISAR imaging is not long, so that it is feasible to approximate the non-uniform rotation of target by uniformly accelerated rotation. According to the radar echo characteristics of non-uniform rotation targets, especially uniformly accelerated rotation targets, ISAR imaging methods based on discrete chirp-Fourier transform (DCFT), fractional Fourier transform (FRFT) and matching Fourier transform (MFT) have been proposed and studied [18–22]. In light of the good energy concentration property of MFT to non-stationary signal, MFT-based ISAR imaging method is discussed in [21, 22], where MFT is utilized for azimuth compression, and only once parameter estimation is needed in the entire imaging process. Inspired by their work and combine with CS principle, we introduce CS into the ISAR imaging problem of non-uniform rotation targets [23]. The major contribution of this paper is that we improve the imaging performance of previous methods for non-uniform rotation targets by more reasonable sparsity analysis and parameter

optimization, especially for the case of limited pulses corresponding to sparse apertures and short apertures.

In Section 2, we introduce the radar echo model of non-uniform rotation targets and analyze the sparsity of range cell echo in matching Fourier domain. In Section 3, we establish the compressive measurement model in azimuth direction, and the restraint condition on the effective measurement matrix for CS reconstruction is checked, including the Restricted Isometry Property (RIP) and incoherence. After that, a CS-based imaging method for non-uniform rotation targets is proposed and the detailed procedures are presented in Section 4. Particularly, in view of the fact that the range cell echo of uniformly accelerated rotation targets is multi-component linear frequency modulation (LFM) signal, and the ratio of the quadratic phase coefficient to the linear phase coefficient is a constant depending on the relative rotation parameter, which must be pre-estimated for the sparse dictionary construction, we propose to estimate the parameter based on the energy concentration property of LFM signal in FRFT domain. In Section 5, the effectiveness of the proposed imaging method and its superiority over traditional methods are demonstrated via simulation experiments. Finally, the whole paper is summed up.

2. RADAR ECHO MODEL OF NON-UNIFORM ROTATION TARGETS AND SPARSITY ANALYSIS

2.1. Radar Echo Model

For analytical simplicity, motion compensation is assumed to have been accomplished. As illustrated in Figure 1, the distance from the target to radar is R_0, the target rotation angle at time t is $\theta(t)$ and $0 \leq t \leq T_{\text{obs}}$, where T_{obs} denotes the CPI. Under the far field assumption, the instantaneous distance from the ith scattering center (x_i, y_i) of the target to radar is given by

$$R_i(t) = R_0 + x_i \sin\theta(t) + y_i \cos\theta(t) \tag{1}$$

Suppose the radar transmits LFM signals with pulse width T_p and band width B, namely

$$S_T\left(\hat{t}, t_m\right) = \text{rect}\left(\frac{\hat{t}}{T_p}\right) \exp\left\{j2\pi\left(f_c t + \frac{1}{2}\gamma\hat{t}^2\right)\right\} \tag{2}$$

where $\text{rect}(\cdot)$ denotes the unit rectangular function, f_c, $\gamma = B/T_p$, $\hat{t}$ and t_m are the carrier frequency, chirp rate, fast-time and slow-time, respectively. Assuming that the target to be imaged consists of P

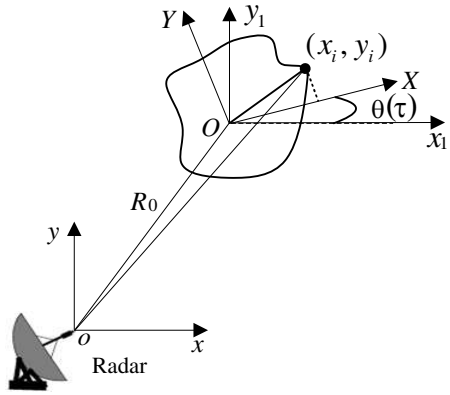

Figure 1. Geometric model of ISAR.

scattering centers, δ_i is the backward scattering intensity of the ith scattering center, then the echoed signal in the range-Doppler domain after range compression can be expressed as

$$S(r,t) = \text{rect}\left(\frac{t}{T_{\text{obs}}}\right)\sum_{i=1}^{P}\delta_i T_p \,\text{sinc}\left\{\frac{2\gamma T_p}{c}[r - x_i\sin\theta(t) - y_i\cos\theta(t)]\right\} \cdot\exp\left\{-j\frac{4\pi}{\lambda}[x_i\sin\theta(t) + y_i\cos\theta(t)]\right\} \quad (3)$$

where c is the light velocity, and $\lambda = c/f_c$ is the wavelength.

Generally, the rotation angle during the CPI satisfies the small angle approximations that $\sin\theta(t) \approx \theta(t)$, $\cos\theta(t) \approx 1$, $\theta(t)$ can be expanded into Taylor series as $\theta(t) = \Omega_0 t + \Omega_1 t^2/2! + \Omega_2 t^3/3! + \ldots$. In most applications, the CPI of ISAR is usually not long, generally several seconds, it is advisable to take the second-order approximation, i.e., the target approximately rotates with a constant acceleration. Suppose the initial angular velocity is Ω_0, the angular acceleration is α, then (3) can be approximated by

$$S(r,t) = \text{rect}\left(\frac{t}{T_{\text{obs}}}\right)\sum_{i=1}^{P}\delta_i T_p \,\text{sinc}\left\{\frac{2\gamma T_p}{c}\left[r - x_i\left(\Omega_0 t + \frac{1}{2}\alpha t^2\right) - y_i\right]\right\} \cdot\exp\left\{-j\frac{4\pi}{\lambda}\left[x_i\left(\Omega_0 t + \frac{1}{2}\alpha t^2\right) + y_i\right]\right\} \quad (4)$$

Assuming that there is no migration through range cell (MTRC) or the MTRC has been removed, the nth range cell contains P_n scattering centers with different cross-range locations, then the echoed signal in

this range cell can be expressed as

$$S_n(t) = \text{rect}\left(\frac{t}{T_{\text{obs}}}\right)\sum_{i=1}^{P_n}\delta_i' \exp\left\{-j\frac{4\pi}{\lambda}x_i\left(\Omega_0 t+\frac{1}{2}\alpha t^2\right)\right\} \tag{5}$$

where $\delta_i' = \delta_i T_p \exp\left\{-j\frac{4\pi}{\lambda}n\Delta r\right\}$, $\Delta r = c/2B$ is the range resolution.

Till now, we establish the radar echo model in the range-Doppler domain of uniformly accelerated rotation targets. As can be noted from (5), the echoed signal in a range cell is the linear superposition of P_n LFM components with center frequency $f_i = -2\Omega_0 x_i/\lambda$ and chirp rate $\mu_i = -2\alpha x_i/\lambda$, each component corresponds to the echoed signal in the range cell from a strong scattering center, and the signal parameter reflects the target rotational characteristic. Both the initial frequency and chirp rate are different for scattering centers with different cross-range locations, which cannot be discriminated by simple Fourier transform (FT). However, both f_i and μ_i are in direct proportion to the scattering center cross-range location x_i, and their ratio satisfies

$$\mu_i/f_i = \alpha/\Omega_0 = \eta_0 \tag{6}$$

2.2. Sparsity Analysis in Matching Fourier Domain

As a generalization of conventional FT, MFT is an effective signal processing tool for non-stationary signal [24, 25], which can achieve energy concentration in matching Fourier domain by selecting a proper basis function. Compared with FT, the key point of MFT lies in that it considers the integral path, also known as the frequency modulation function. The same signal has distinct transform results with respect to different integral paths, i.e., the projections of the same signal in different orthogonal systems are dissimilar. The signal energy can be concentrated in the matching Fourier spectrum only when the integral path matches well with the signal.

Let $\omega_i = \frac{4\pi}{\lambda}x_i\Omega_0$, $\phi(t) = t + \frac{1}{2}\eta_0 t^2$, then $\phi(t)$ is a monotonously bounded function and $\phi(0) = 0$. Taking $\phi(t) = t + \eta_0 t^2/2$ as the integral path, the MFT of $S_n(t)$ is given by

$$S_n(\omega) = \int_0^{T_{\text{obs}}} \text{rect}\left(\frac{t}{T_{\text{obs}}}\right)\sum_{i=1}^{P_n}\delta_i' \exp\{-j(\omega_i+\omega)\phi(t)\}(1+\eta_0 t)\,dt \tag{7}$$

According to the linear property of MFT and let $f_d = \omega/2\pi$, we

can get

$$S_n(f_d) = \sum_{i=1}^{P_n} \delta_i' \cdot \phi(T_{\text{obs}}) \cdot \text{sinc}\left[\phi(T_{\text{obs}})\left(f_d + \frac{2x_i\Omega_0}{\lambda}\right)\right] \cdot \exp\left\{-j\pi\left(f_d + \frac{2x_i\Omega_0}{\lambda}\right)\phi(T_{\text{obs}})\right\} \quad (8)$$

Obviously, $S_n(t)$ is transformed into sinc pulses with a narrow width of $1/\phi(T_{\text{obs}})$ by MFT and achieves energy concentration. The cross-range distribution of the target reflectivity can be determined from peak positions of the sinc pulses, the peak value position f_{di} and the scattering center cross-range location x_i satisfy $x_i = -f_{di} \cdot \lambda/2\Omega_0$, so the corresponding azimuth resolution is $\Delta x = \lambda/(2\theta(T_{\text{obs}}))$, where $\theta(T_{\text{obs}}) = \Omega_0\phi(T_{\text{obs}})$ is the total rotation angle during the CPI. Therefore, the azimuth resolution of MFT method is consistent with conventional Range-Doppler (RD) algorithm. Consequently, the representation of range cell echo in certain matching Fourier domain can characterize the cross-range distribution of the target reflectivity. In other words, the echoed signal in the range-Doppler domain of uniformly accelerated rotation targets is sparse in matching Fourier domain, and each component corresponds to a prominent scattering center in the range cell.

To facilitate the forthcoming analysis, we prefer to express the echo model in matrix form. Denoting the vector form of $S_n(t)$ as $\mathbf{s}_n$, $\boldsymbol{\sigma}$ is the sparse coefficient of s_n in matching Fourier domain and represents the spatial distribution of the target scattering centers in the nth range cell. Let $\mathbf{F}_\eta$ be the normalized MFT matrix, then

$$\mathbf{F}_\eta \mathbf{s}_n = \boldsymbol{\sigma} \quad (9)$$

The basis function set $\{e^{-j\omega\phi(t)}\}$ of MFT is orthogonal after taking the integral path into consideration [25], and the existence of the matching Fourier orthogonal set ensures that the interested signal can achieve energy concentration by MFT. As the discrete MFT takes the integral path into account, the corresponding MFT matrix is approximately orthogonal, hence $\mathbf{F}_\eta^H \mathbf{F}_\eta \approx \mathbf{I}$, $\mathbf{F}_\eta^H \approx \mathbf{F}_\eta^{-1}$, where $\mathbf{F}_\eta^H$ denotes the conjugate transpose matrix of $\mathbf{F}_\eta$. Then, (9) can be recast as

$$\mathbf{s}_n = \mathbf{F}_\eta^H \boldsymbol{\sigma} = \boldsymbol{\Psi}\boldsymbol{\sigma} \quad (10)$$

where $\boldsymbol{\Psi} = \mathbf{F}_\eta^H$ is just the sparse dictionary of range cell echo $\mathbf{s}_n$. In essence, it means that $\boldsymbol{\Psi}$ transforms the sparsity in Doppler domain into a sparse vector via MFT operation.

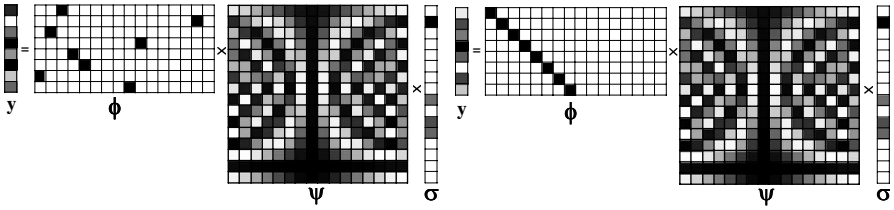

(a) (b)

Figure 2. Linear measurement sketches of sparse aperture and short aperture data. (a) Sparse aperture case. (b) Short aperture case.

3. COMPRESSIVE DATA ACQUISITION AND MEASUREMENT MATRIX EVALUATION

The state-of-art multifunction radar system usually provides gapped and short interval observation, the corresponding sampling pattern in Doppler domain can be considered in the construction of the azimuth sparse dictionary [13], thereby the super-resolution image can be obtained via CS algorithm. Suppose the compressive sampling matrix is $\mathbf{\Phi}$, in the short aperture case, the action of $\mathbf{\Phi}$ is equivalent to selecting partial rows of $\mathbf{\Psi}$ in series, thus $\mathbf{\Phi}$ is a matrix consisting of partial sequential rows of an identity matrix. In the random sparse aperture case, the action of $\mathbf{\Phi}$ is equivalent to selecting partial rows of $\mathbf{\Psi}$ randomly, thus $\mathbf{\Phi}$ is a matrix consisting of partial random rows of an identity matrix. Figure 2 illustrates the linear measurement process in both cases of sparse aperture and short aperture. Assuming that the noise vector in the nth range cell is $\mathbf{n}$, then the compressive measurement model can be expressed as

$$\mathbf{y}_n = \mathbf{\Phi}\mathbf{\Psi}\boldsymbol{\sigma} + \mathbf{n} = \mathbf{\Phi}\mathbf{F}_\eta^H\boldsymbol{\sigma} + \mathbf{n} = \mathbf{\Theta}\boldsymbol{\sigma} + \mathbf{n} \tag{11}$$

where $\mathbf{\Theta} = \mathbf{\Phi}\mathbf{\Psi} = \mathbf{\Phi}\mathbf{F}_\eta^H$ denotes the effective measurement matrix, also called reconstruction matrix. Here $\mathbf{\Theta}$ is a partial matching Fourier matrix with more columns than rows in essence.

CS theory indicates that, when $\mathbf{\Theta}$ obeys the so-called RIP or incoherence condition, the target reflectivity distribution $\boldsymbol{\sigma}$ in a range cell can be recovered by resolving the ℓ_1 norm minimization problem with relaxation constraint as follows:

$$\hat{\boldsymbol{\sigma}} = \arg\min \|\boldsymbol{\sigma}\|_1 \quad \text{s.t.} \quad \|\mathbf{y} - \mathbf{\Theta}\boldsymbol{\sigma}\|_2 \leq \varepsilon \tag{12}$$

where ε is a threshold determined by the noise level. Designing a sensing matrix $\mathbf{\Phi}$ such that the resulting effective measurement matrix $\mathbf{\Theta} = \mathbf{\Phi}\mathbf{\Psi}$ has the RIP is a fundamental problem in CS. Both random Gaussian matrix and partial Fourier matrix are well known to obey

the RIP with high probability under certain sparsity condition [11, 26]. To check the validity and stability of the CS-based imaging method using limited pulse echo, the RIP and incoherence of matrix $\mathbf{\Theta}$ should be evaluated in priority.

A matrix $\mathbf{\Theta}$ is said to satisfy the RIP of order K with the Restricted Isometry Constants (RIC) $\delta_K \in (0, 1)$ if

$$(1 - \delta_K) \|\mathbf{v}\|_2^2 \leq \|\mathbf{\Theta v}\|_2^2 \leq (1 + \delta_K) \|\mathbf{v}\|_2^2 \tag{13}$$

for any K-sparse signal $\mathbf{v}$ ($\|\mathbf{v}\|_0 \leq K$). The RIP essentially states that all subsets of K columns taken from $\mathbf{\Theta}$ are in fact nearly orthogonal, and the smaller the RIC, the better the approximation. A related condition is known as incoherence. The incoherence of $\mathbf{\Theta}$ requires that the rows of $\mathbf{\Phi}$ cannot sparsely represent the columns of $\mathbf{\Psi}$ and vice versa, it can be measured by the mutual coherence μ which is defined as the maximum of the correlation coefficients between any two normalized columns of $\mathbf{\Theta}$ [27]. Equivalently, once the columns of $\mathbf{\Theta}$ have been normalized, μ can be viewed as the largest off-diagonal entry of the Gram matrix $\mathbf{G} = \mathbf{\Theta}^H \mathbf{\Theta}$. Generally, smaller μ is propitious to sparse recovery, the matrix $\mathbf{\Theta}$ is said to be incoherent when μ is small.

Suppose the support of a K-sparse signal $\mathbf{v} \in \mathbb{C}^M$ is Ω, and $\mathbf{\Theta}_\Omega$ is a submatrix of $\mathbf{\Theta}$ containing only partial columns of $\mathbf{\Theta}$ indexed by Ω. Theoretically, to check whether $\mathbf{\Theta}$ satisfies K-RIP, we need to check whether the eigenvalues of $\mathbf{\Theta}_\Omega^H \mathbf{\Theta}_\Omega$ are in the interval $(1 - \delta_K, 1 + \delta_K)$ (sufficiently close to 1) for all C_M^K possible Ω, which is computationally difficult. To facilitate analysis, considering the signal rather than the measurements stochastically, we take the statistical average value of the extremal eigenvalues of $\mathbf{\Theta}_\Omega^H \mathbf{\Theta}_\Omega$ as a quality measure as in [26]. Suppose the dimension of the sparse signal to be recovered is $M = 256$, the available sample amount is 64, then the size of corresponding $\mathbf{\Theta}$ is 64×256. We perform 1000 Monte Carlo trials to analyze the eigenvalue statistics of $\mathbf{\Theta}_\Omega^H \mathbf{\Theta}_\Omega$, the means of the maximum and minimum eigenvalues of $\mathbf{\Theta}_\Omega^H \mathbf{\Theta}_\Omega$ for varying K is shown in Figure 3(a), and different sets Ω are generated uniformly random over all C_M^K sets for every value K. For comparison, the statistical results of random Gaussian matrix and partial Fourier matrix are also given. Thereinto, 'MFT1' and 'MFT2' respectively represent the partial matching Fourier matrices under the circs of sparse aperture and short aperture, 'Gaussian' denotes the random matrix with Gaussian entries of zero mean and 1/64 variance, while 'FT1' and 'FT2' correspond to the partial Fourier matrices in the sparse aperture and short aperture cases [10, 15], respectively.

As seen from Figure 3(a), our partial matching Fourier matrix has similar statistical results to partial Fourier matrix, this implies

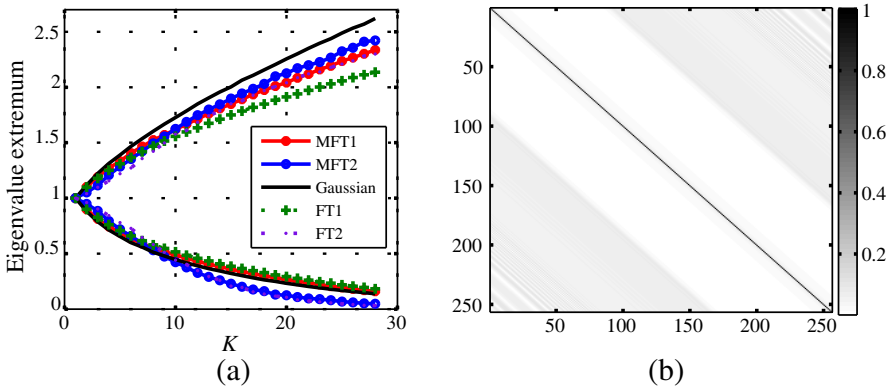

Figure 3. Analysis on the constraint condition of CS reconstruction. (a) Eigenvalue statistics of $\boldsymbol{\Theta}_{\Omega}^{H}\boldsymbol{\Theta}_{\Omega}$. (b) Autocorrelation matrix of $\boldsymbol{\Psi}$.

they have similar RIP property. Moreover, the eigenvalues of $\boldsymbol{\Theta}_{\Omega}^{H}\boldsymbol{\Theta}_{\Omega}$ with respect to MFT matrix and FT matrix are, on average, closer to 1 compared to the Gaussian measurement case, which means that smaller RICs can be obtained in a statistic sense. As a special case, Figure 3(a) tell us that when $|\Omega| \leq 18$, the deviations of the eigenvalue statistics from one with respect to MFT matrix and FT matrix are smaller than 1, while the critical condition in Gaussian case is $|\Omega| \leq 15$. Therefore, if Gaussian matrix satisfy any K-RIP condition, our $\boldsymbol{\Theta}$ will also be able to recover a random K-sparse signal with high probability.

To check the incoherence of $\boldsymbol{\Theta}$, the autocorrelation matrix of the sparse dictionary $\boldsymbol{\Psi}$ is computed and depicted in Figure 3(b). Notably, the autocorrelation matrix is close to an identity matrix, of which the diagonal entries are dominant, this fact means that $\boldsymbol{\Psi}$ is approximately orthogonal and satisfies the constraint condition of signal recovery from a small number of measurements, the corresponding $\boldsymbol{\Theta}$ is essentially a kind of subsampled incoherent bases that can be used as a CS reconstruction matrix [28].

4. RADAR IMAGE FORMATION

4.1. Parameter Estimation

ISAR targets are often noncooperative, the rotation parameters cannot be obtained directly so as to determine the optimal integral path. From the analysis in Subsection 2.2, only the relative rotation parameter η_0 is required to define $\phi(t)$, i.e., as long as the phase coefficients of the echoed signal from a certain scattering center are estimated, η_0 can

be calculated to determine $\phi(t)$. For our specific case of imaging with limited pulses corresponding to short apertures and sparse apertures, the range cell echo data is length limited and/or incontinuous, we propose to perform the detection and estimation of LFM signal via sparse component analysis, then the relative rotation parameter can be calculated and utilized to construct the MFT dictionary.

As a novel time-frequency analysis method, the completely time-domain analysis and linear transform property of FRFT make it having particular superiority in the processing of LFM signal [29]. FRFT can be viewed as a rotation of the time-frequency plane, the rotation angle α and the transform order p satisfy $\alpha = p\pi/2$. The FRFT of a LFM signal with finite length can achieve the best energy concentration in a proper fractional Fourier domain, this property has already been used in the separation of multi-component LFM signal [19]. As mentioned before, the range cell echo of uniformly accelerated rotation targets with multiple scattering centers is multi-component LFM signal, and both the initial frequency and chirp rate of each component are different, thereby appears as multiple noncrossing slant lines in the time-frequency plane, the echoed signal corresponding to each scattering center will concentrate to a peak of sinc function in the fractional frequency spectrum perpendicular to it. When one component achieves the best energy concentration in a certain fractional Fourier domain, the energy of other components will disperse, as shown in Figure 4. For clarity purpose, only the projections with the optimal energy concentration in the fractional frequency domain u_1 and u_2 are depicted.

In fact, we only need to estimate the LFM signal parameters of a strong scattering center in a range cell, i.e., estimate the LFM

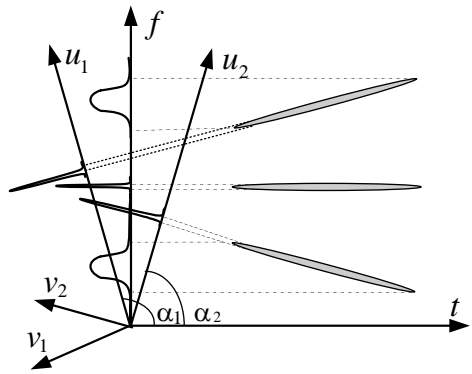

Figure 4. FT and FRFT sketch of range cell echo data.

parameters of the strongest component. The energy concentration property of LFM signal in fractional Fourier domain can be measured by the fourth-order origin moment of the fractional frequency spectrum, the better the energy concentration, the larger the origin moment. Therefore, given the rotation angle or transform order interval within which we perform parameter optimization, the optimal rotation angle α_0 can be found taking the maximum origin moment of the recovered fractional spectrum as search criteria, thus the chirp rate estimation is $\hat{\mu} = -\cot\alpha_0$. Afterwards, the peak value position of the obtained fractional spectrum is searched to get the initial frequency $\hat{f}_0 = u/\sin\alpha_0$, accordingly the relative rotation parameter $\hat{\eta}_0 = \hat{\mu}\Big/\hat{f}_0$. Note that there is a tradeoff between computation complexity and search precision, the golden section method [30] is adopted for efficiency purpose in this paper.

4.2. Imaging Process

Once the relative rotation parameter $\hat{\eta}_0$ is obtained, we substitute it into $\phi(t)$ to determine the optimal integral path, then the MFT dictionary can be constructed, and the azimuth compression can be realized via nonlinear optimization. Taking both the operation efficiency and reconstruction precision into consideration, we adopt the smoothed L0 (SL0) algorithm [31] in the following experiments, and the superiority of matrix operation of SL0 algorithm in multiple sparse recovery is utilized for efficiency purpose.

To avoid the estimation error of $\hat{\eta}_0$ getting too large and improve the reconstruction performance, we take the result of FT dictionary [10] as a comparison and make adjustment in time. In theory, since our MFT dictionary matches better with the echo model of non-uniform rotation targets, its result is superior to, or at least comparable with the result of FT dictionary, otherwise, we are again in a demand to select a new range cell to estimate the parameter η_0. If the reconstruction result is relatively preferable, we proceed with further search within a small range around $\hat{\eta}_0$, and choose the optimal result as our final imaging output. In the comparison process, the sparsity of the reconstructed cross-range profile measured by ℓ_1 norm is taken as a quality metric, the smaller the ℓ_1 norm, the sparser the reconstruction result.

In summary, the proposed CS-based imaging method for non-uniform rotation targets can be described as follows:

1) Preprocessing. With the limited pulse echo data after range compression and motion compensation, construct the FT dictionary $\mathbf{F}$ and calculate the corresponding effective measurement matrix $\tilde{\mathbf{\Theta}} =$

$\mathbf{\Phi F}$, then perform azimuth compression via SL0 algorithm and store the result for the comparison in step 4).

2) Parameter estimation. Choose a certain range cell and estimate the strongest LFM component parameters based on the sparse representation in FRFT domain, thereby determine the relative rotation parameter $\hat{\eta}_0$.

3) Azimuth compression. Construct the MFT dictionary $\mathbf{F}_{\eta}^{H}$ in light of $\hat{\eta}_0$, and perform azimuth compression via SL0 algorithm with the effective measurement matrix $\mathbf{\Theta} = \mathbf{\Phi F}_{\eta}^{H}$.

4) Comparison processing. Compare the energy concentration effect with the result in step 1), if the result corresponding to $\mathbf{F}_{\eta}^{H}$ is inferior, go back to step 2) and select a new range cell, otherwise, proceed with the next step.

5) Refined optimal search. Set a small change range around $\hat{\eta}_0$ and search the optimal reconstruction result further within the refined interval, take the sparsest result as the output, consequently a clear ISAR image is obtained from limited pulses.

It is worth pointing out that, since the MTRC of scattering center may occur and different targets have diverse reflectivity distribution, the rotation parameter estimation approach by directly selecting a certain range cell needs the active participation of human. We can consult the idea in [18] and estimate η_0 based on all echo data, i.e., integrate (4) with respect to the radial range r, and then proceed based on the integrated result. In practical implementations, the proposed algorithm maintains the insensitivity of traditional MFT-based imaging method [22] to the parameter estimation precision, thus step 5) often can be omitted.

5. SIMULATION EXPERIMENTS

Here we use both simulated data and measured data in anechoic chamber to verify the effectiveness of the proposed imaging method. For simplicity, conventional FFT method is utilized for range compression in the following simulations, the difference among different imaging schemes mainly lies in the azimuth direction processing.

5.1. Simulated Data

Suppose the radar transmits LFM signals with carrier frequency 10 GHz, bandwidth 1 GHz and pulsewidth 100 μs, the pulse repetition frequency is 400 Hz, the sampling amount within a pulse time is 256, amounting to 256 transmitted pulses. As shown in Figure 5(a), the simulated target consists of 16 scattering centers with a uniform

intensity, it rotates with an initial angular velocity of $\Omega_0 = 0.15\,\mathrm{rad/s}$ and an acceleration of $\alpha = 0.45\,\mathrm{rad/s}^2$, then $\eta_0 = 3$. In addition, we add complex white Gaussian noise to the simulated radar echoes, the signal-to-noise ratio (SNR) is 15 dB.

Figure 5(b) shows the imaging result of traditional RD method with the full aperture data, Figures 5(c) and (d) present the results of MFT-based method with the full aperture and 1/4 short aperture data, respectively, and the rotation parameters are assumed to be known exactly in both cases. Notably, the ISAR image produced by RD algorithm is heavily defocused in the cross-range direction, and the farther the scattering center away from the rotating center, the severer the defocusing and distortion effect. This fact occurs as

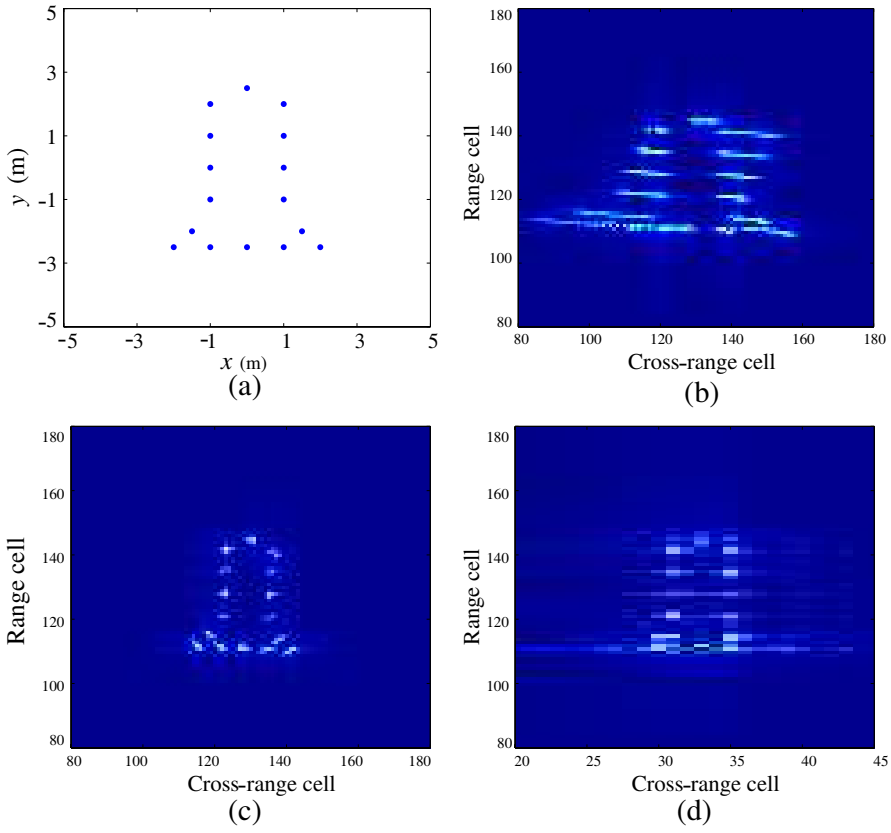

Figure 5. Simulated target model and imaging results of traditional methods. (a) Simulated target model. (b) Full aperture RD imaging. (c) Full aperture MFT imaging. (d) Short aperture MFT imaging.

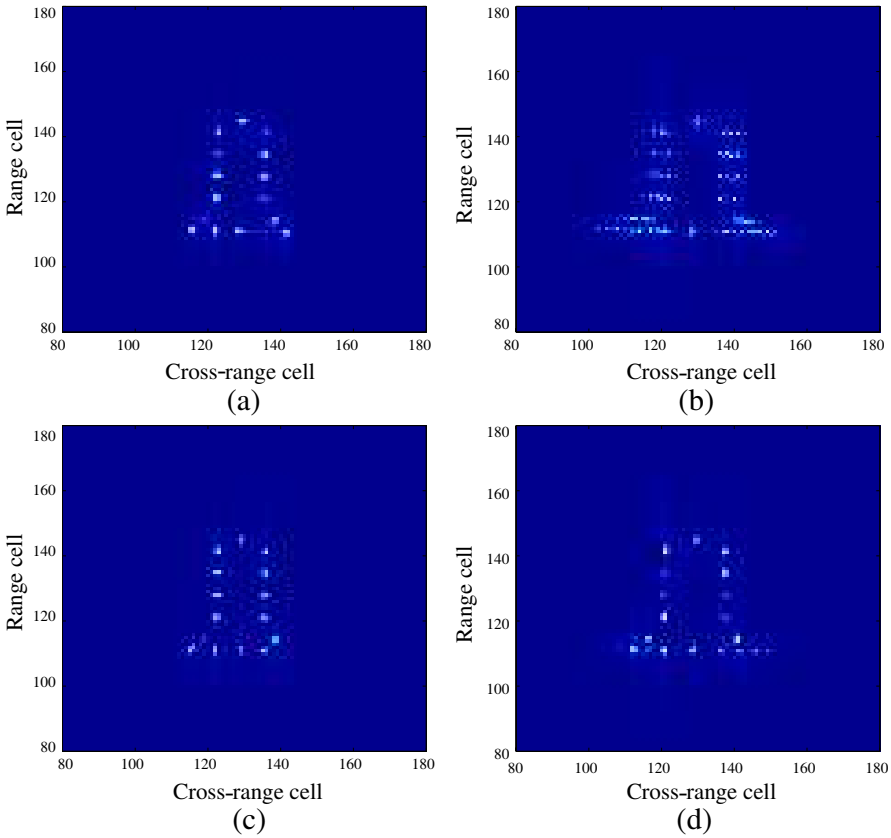

Figure 6. CS-based imaging results of the simulated target with sparse aperture and short aperture data. (a) Sparse case with MFT dictionary. (b) Sparse case with FT dictionary. (c) Short case with MFT dictionary. (d) Short case with FT dictionary.

a result of the Doppler time-varying property of scattering centers induced by the non-uniform rotation of the target. In contrast, the ISAR image obtained by MFT method focuses very well and has remarkably improved quality. However, except for the demand of parameter estimation, MFT method also requires sufficient pulses to get high azimuth resolution. When the effective aperture is sparse or short, MFT method cannot achieve the expected result, and even become invalid in the sparse aperture case. Due to space limitations, the completely distorted imaging result with respect to sparse aperture is not displayed.

To verify the effectiveness of the proposed CS-based imaging

method for non-uniform rotation targets, suppose that part of the transmitted 256 pulses are missed and only the echo data from 64 wideband pulses are collected randomly. The CS reconstruction results based on MFT dictionary and FT dictionary are shown in Figures 6(a) and (b), respectively, where the parameter estimation $\hat{\eta}_0 = 3.1769$. Figures 6(c) and (d) present the CS results based on the two sparse dictionaries with the short aperture data of 64 continuous pulses, respectively, where the parameter estimation $\hat{\eta}_0 = 2.9831$. As can be seen, the proposed method can achieve high azimuth resolution with limited number of pulses, the scattering center distribution in the image correctly reflects the actual distribution of the target reflectivity. Both CS-based methods with the two dictionaries can overcome the defocusing effect in azimuth direction of non-uniform rotation targets. However, there is a cross-range scaling in the results of CS method with FT dictionary due to its mismatch to the target echo model, while the results of our method which matches better with the target motion model are more preferable in comparison. In addition, as traditional FFT method is used for range compression, relative high side lobes appear in the range direction, while CS-based method avoids the problem of high side lobes accompanying traditional methods effectively.

To compare the imaging performance of our CS-based method with several traditional methods more visually, the profiles of the 111th range cell of the imaging results are shown in Figure 7, where FFT method and MFT method utilize the full aperture data (since traditional methods cannot get well-focused results with limited pulse

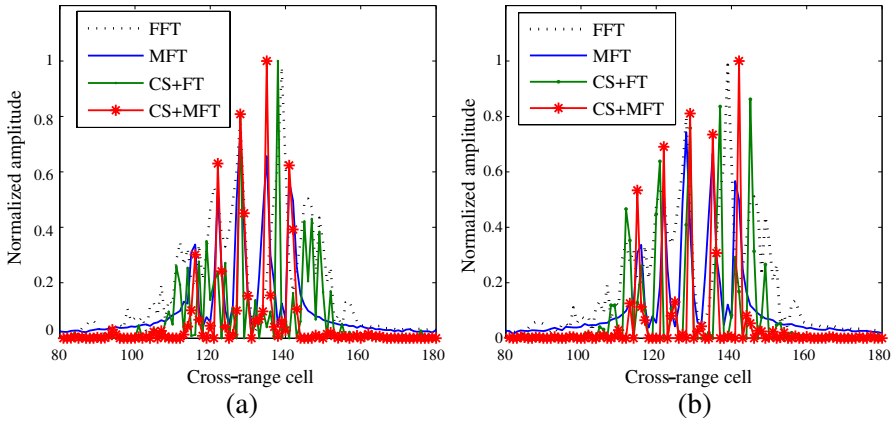

Figure 7. Range cell profiles of azimuth compression. (a) Random sparse aperture. (b) Continuous short aperture.

data), while both CS-based methods utilize 1/4 pulse echo data. From the comparison, we can find that the CS-based methods have better side-lobe suppression effect than traditional methods, and the reconstruction result of the proposed method is more consistent with the target reflectivity, thus it can get more focused ISAR image even with less measurement data.

5.2. Measured Data

The observation radar in anechoic chamber operates in the frequency scanning mode, and its work frequency ranges from 8 GHz to 12 GHz with a step size of 20 MHz. As shown in Figure 8(a), the measured target is a scaled model of warhead, the pitching angle is 0°, and the azimuth angle varies from 0° to 90° with a step size of 0.2°. Suppose

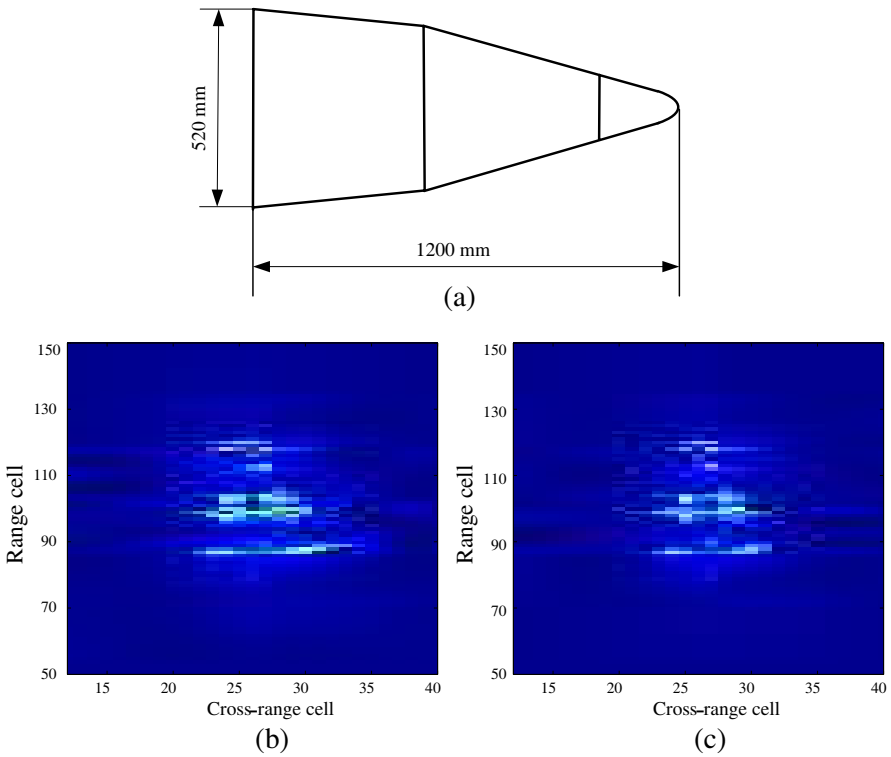

Figure 8. Measured target model and imaging results of traditional methods. (a) Outline of the measured target. (b) RD imaging. (c) MFT imaging.

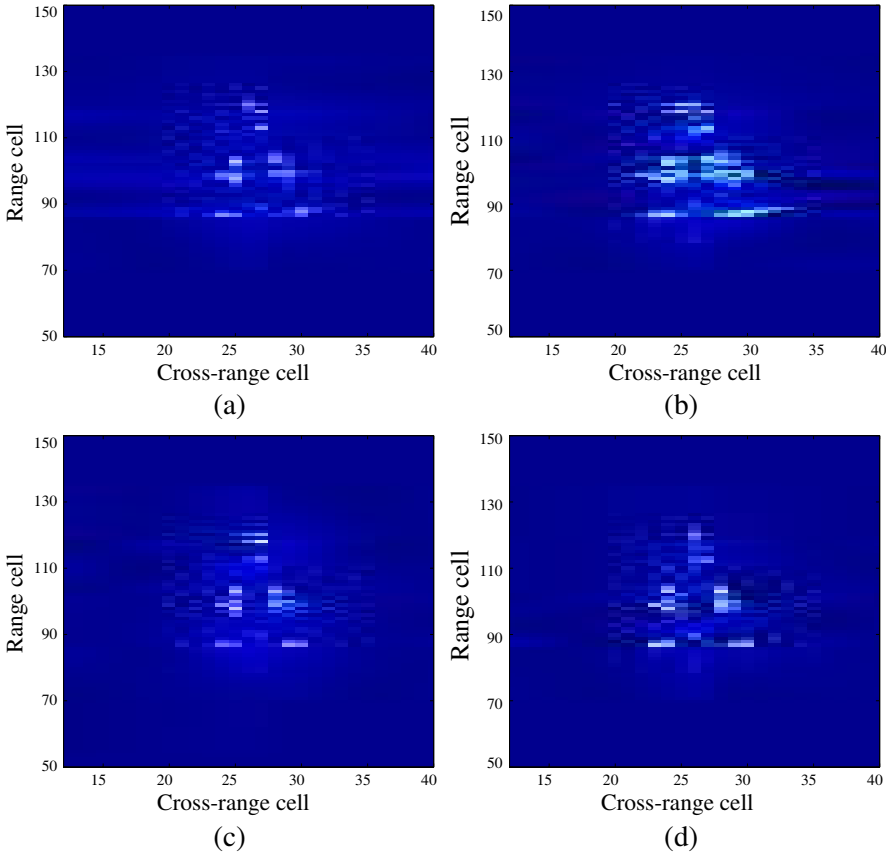

Figure 9. CS-based imaging results of the measured target with sparse aperture and short aperture data. (a) Sparse case with MFT dictionary. (b) Sparse case with FT dictionary. (c) Short case with MFT dictionary. (d) Short case with FT dictionary.

that the initial azimuth angle is 0°, the target rotation parameters are $\Omega_0 = 1\,\text{rad/s}$ and $\alpha = 4\,\text{rad/s}^2$, then $\eta_0 = 4$. The sampling frequency in azimuth direction is 300, amounting to 51 pulses, thus the total rotation angle is 12.7°. Figures 8(b) and (c) illustrate the imaging results of traditional RD method and MFT method with the full aperture data. As shown, owing to the non-uniform sampling in cross-range induced by non-uniform rotation, the defocusing phenomenon occurs in azimuth direction of the RD image, while MFT method takes the non-uniform rotation into consideration, better focusing result is obtained, but there still exist relatively high side lobes.

The imaging results of CS methods based on the two sparse dictionaries in the sparse aperture and short aperture cases are given in Figure 9, where only 26 pulses are used for imaging. Obviously, the CS-based imaging method can achieve high azimuth resolution with limited pulse echo data. By contrast, the reconstruction results corresponding to MFT dictionary exceed the results of FT dictionary in quality, especially in the circs of sparse aperture, the target reflectivity distribution in the image obtained by our method is more explicit, and has less background clutters, which is beneficial to feature extraction and target recognition. The conventional FT dictionary has better results in the short aperture case than the sparse aperture case, this is because that the target motion characteristic can be simplified properly in the short aperture case. Consequently, the results of anechoic chamber data verify the effectiveness and superiority of the proposed method for non-uniform rotation targets.

It should be noted that, since the azimuth sampling interval (0.2°) of the measured data in anechoic chamber is relatively large, the equivalent sampling points of the target with non-uniform rotation may be off the measurement points in overwhelming probability, thereby most sampling points are taken approximation processing, which inevitably will bring some errors to the synthesized data. These errors produced by approximation processing may not have negative influence on traditional imaging methods, but will make the performance of the proposed method degrade in a certain extent, because the corresponding echo model varies slightly.

6. CONCLUSIONS

The non-uniform rotation of ISAR targets can be reasonably approximated by uniformly accelerated rotation during the CPI. In light of the superiority of CS on processing sparse or compressible signal, a novel strategy for ISAR imaging of non-uniform rotation targets with limited pulses has been studied in this paper. The sparsity of the range cell echo in certain matching Fourier domain is analyzed, then the RIP and incoherence of the corresponding effective measurement matrix are checked, after which a CS-based ISAR imaging method is proposed. As the sparse dictionary for reconstruction depends on the relative rotation parameters of radar target, in view of the fact that the range cell echo of uniformly accelerated rotation targets is multi-component LFM signal, and the energy concentration property of FRFT to LFM signal, a parameter estimation method based on sparse representation and optimal search is presented. Compared to the existing imaging methods for non-

uniform rotation targets, the proposed method can achieve high azimuth resolution with sparse aperture or short aperture data, it performs better in terms of imaging performance, and can be easily extended to targets with higher order rotation motion. The difference lies in that the polynomial phase coefficients of the echoes of a strong scattering center should be estimated in advance, which can be implemented by choosing a proper basis function and incorporating evolution algorithms. However, there are still many issues need further study, such as lower computational efficiency and higher sensitivity to the signal-to-noise ratio for the current Algorithms.

ACKNOWLEDGMENT

This work was supported by the National Natural Science Foundation of China for Distinguished Young Scientists (Grant No. 61025006) and National Natural Science Foundation of China (Grant No. 61171133).

REFERENCES

1. Bao, Z., M. D. Xing, and T. Wang, *Radar Imaging Technique*, Publishing House of Electronics Industry, Beijing, 2006.
2. Donoho, D. L., "Compressed sensing," *IEEE Trans. Inform. Theory*, Vol. 52, No. 4, 1289–1306, 2006.
3. Candes, E. and M. Wakin, "An introduction to compressive sampling," *IEEE Sig. Proc. Mag.*, Vol. 25, No. 2, 21–30, 2008.
4. Ender, J. H. G., "On compressive sensing applied to radar," *Signal Processing*, Vol. 90, No. 5, 1402–1414, 2010.
5. Potter, L. C., E. Ertin, J. T. Parker, and M. Cetin, "Sparsity and compressed sensing in radar imaging," *Proceedings of the IEEE*, Vol. 98, No. 62, 1006–1020, 2010.
6. Wei, S.-J., X.-L. Zhang, and J. Shi, "Linear array SAR imaging via compressed sensing," *Progress In Electromagnetics Research*, Vol. 117, 299–319, 2011.
7. Wei, S.-J., X.-L. Zhang, J. Shi, and G. Xiang, "Sparse reconstruction for SAR imaging based on compressed sensing," *Progress In Electromagnetics Research*, Vol. 109, 63–81, 2010.
8. Chen, J., J. Gao, Y. Zhu, W. Yang, and P. Wang, "A novel image formation algorithm for high-resolution wide-swath spaceborne SAR using compressed sensing on azimuth displacement phase center antenna," *Progress In Electromagnetics Research*, Vol. 125, 527–543, 2012.

9. Li, J., S. Zhang, and J. Chang, "Applications of compressed sensing for multiple transmitters multiple azimuth beams SAR imaging," *Progress In Electromagnetics Research*, Vol. 127, 259–275, 2012.
10. Zhang, L., M. D. Xing, C. W. Qiu, J. Li, and Z. Bao, "Achieving higher resolution ISAR imaging with limited pulses via compressed sampling," *IEEE Geosci. Remote Sens. Lett.*, Vol. 6, No. 3, 567–571, 2009.
11. Zhang, L., M. D. Xing, C. W. Qiu, et al., "Resolution enhancement for inversed synthetic aperture radar imaging under low SNR via improved compressive sensing," *IEEE Trans. Geosci. Remote Sens.*, Vol. 48, No. 10, 3824–3838, 2010.
12. Rao, W., G. Li, X. Q. Wang, and X.-G. Xia, "ISAR imaging of maneuvering targets with missing data via matching pursuit," *Proceedings of IEEE Radar Conference*, 124–128, Kansas City, Missouri, USA, 2011.
13. Quan, Y. H., L. Zhang, R. Guo, M. D. Xing, and Z. Bao, "Generating dense and super-resolution ISAR image by combining bandwidth extrapolation and compressive sensing," *SCIENCE CHINA Information Sciences*, Vol. 54, No. 10, 2158–2169, 2011.
14. Zhao, G. H., Z. Y. Wang, Q. Wang, G. M. Shi, and F. F. Shen, "Robust ISAR imaging based on compressive sensing from noisy measurements," *Signal Processing*, Vol. 92, No. 1, 120–129, 2012.
15. Li, J., M. D. Xing, and S. J. Wu, "Application of compressed sensing in sparse aperture imaging of radar," *Proceedings of 2nd Asian-Pacific Conf. on Synthetic Aperture Radar (APSAR'09)*, 1119–1122, Xi'an, China, Oct. 2009.
16. Raghu, G. R. and F. Masoud, "ISAR imaging in sea clutter via compressive sensing," *International Conference on Waveform Diversity and Design Conference (WDD)*, 200–205, Niagara Falls, ON, Aug. 2010.
17. Raghu, G. R., C. C. Victor, and L. Ronald, "A greedy approach for sparse angular aperture radar," *Proceedings of IEEE Radar Conference*, 673–677, Washington, DC, 2010.
18. Fu, Y. W., J. M. Hu, and X. Li, "ISAR imaging of uniform accelerative rotating targets based on chirp-Fourier transform," *Systems Engineering and Electronics*, Vol. 33, No. 12, 2608–2612, 2011.
19. Yin, Z. P., "Applications of fractional Fourier transform to inverse synthetic aperture radar imaging processing," Ph.D. thesis, University of Science and Technology of China, Hefei, 2008.

20. Liu, A. F., X. H. Zhu, J. H. Lu, and Z. Liu, "Imaging in inverse synthetic aperture radar (ISAR) based on discrete matching Fourier transform," *Acta Armamentarii*, Vol. 25, No. 4, 458–462, 2004.
21. Huang, Y. J., M. Cao, Y. W. Fu, Y. N. Li, and W. D. Jiang, "ISAR imaging of equably accelerative rotating targets based on matching Fourier transform," *Signal Processing*, Vol. 25, No. 6, 864–867, 2009.
22. Cao, M., "Research on high resolution radar imaging technology for space targets," Ph.D. thesis, National University of Defense Technology, Changsha, 2009.
23. Liu, J. H., X. Li, Y. L. Qin, and Z. W. Zhuang, "ISAR imaging of non-uniform rotation targets via compressed sensing based on sparsity in matching fourier domain," *1st International Workshop on Compressed Sensing applied to Radar*, Bonn, Germany, May 2012.
24. Wang, S. L., S. G. Li, J. L. Ni, and G. Y. Zhang, "A new transform — Match Fourier transform," *Acta Electronica Sinica*, Vol. 29, No. 3, 403–405, 2001.
25. Wang, S. L., "A new method for radar signal processing-matched Fourier transform," Ph.D. thesis, Xidian University, Xi'an, 2003.
26. Applebaum, L., S. Howard, S. Searle, and R. Calderbank, "Chirp sensing codes: Deterministic compressed sensing measurements for fast recovery," *Applied and Computational Harmonic Analysis*, Vol. 26, No. 2, 283–290, 2009.
27. Patel, V. M., G. R. Easley, D. M. Healy, and R. Chellappa, "Compressed synthetic aperture radar," *IEEE Journal of Selected Topics in Signal Processing*, Vol. 4, No. 2, 244–254, 2010.
28. Duarte, M. F., Y. C. Eldar, and R. Chellappa, "Structured compressed sensing: From theory to applications," *IEEE Trans. Signal Process.*, Vol. 59, No. 9, 4053–4085, 2011.
29. Saxena, R. and K. Singh, "Fractional Fourier transform: A novel tool for signal processing," *J. Indian Inst. Sci.*, Vol. 85, 11–26, 2005.
30. Gerald, C. F. and P. O. Wheatley, *Applied Numerical Analysis*, 7th Edition, Pearson/Addison-Wesley, 2004.
31. Mohimani, H., M. Babaie-Zadeh, and C. Jutten, "A fast approach for overcomplete sparse decomposition based on smoothed l0 norm," *IEEE Trans. Signal Process.*, Vol. 57, No. 1, 289–301, 2009.